Solid State Science and Technology, Vol. 22, No 1 & 2 (2014) 139-147
ISSN 0128-7389 | *http://journal.masshp.net*

OBSERVATION OF DIELECTRIC AND MAGNETIC POLARIZATIONS IN $Ni_{0.3}Zn_{0.7}Fe_2O_4$ VIA COMPLEX-PLANE PLOTS

A.R.Norailiana [1,*], M. Hashim[1, 2], M.I. Fadzidah[2], I. Ismayadi[2], I.R. Idza[1], N. Rodziah[1], A.N. Hapishah[1], M.S.E. Shafie[2], G.H. Bahmanrokh[1], M. Masni[1], M. Masoudi[2]

[1]*Department of Physics, Universiti Putra Malaysia, 43400, Serdang, Selangor.*

[2]*Advanced Materials and Nanotechnology Laboratory, Institute of Advanced Technology, Universiti Putra Malaysia, 43400, Serdang, Selangor.*

Corresponding author: wannorailiana@gmail.com

ABSTRACT

Studies in dielectrics have been carried out for decades and have been numerously reported in the literature such as the frequency response of dielectric component, ε', ε'' and the well known cole-cole plot in which ε'' is plotted against ε'. Hence, guided by the dielectric cole-cole plot, we have proposed to study the magnetic parameter variation of μ'' vs μ'. Polycrystalline nickel zinc ferrite of composition $Ni_{0.3}Zn_{0.7}Fe_2O_4$ has been prepared by using the conventional solid state method. The frequency dependence of the dielectric constant, ε', and the dielectric loss, ε'', were determined in the frequency range from 1MHz to 1GHz for disc-shaped samples sintered at different temperatures: 1260°C, 1300°C and 1340°C. Dielectric complex-plane permittivity plots are now reported as the relation between the dielectric loss, ε'', and the dielectric constant, ε', over the entire frequency range. The real part of magnetic permeability, μ', and the imaginary part of the permeability, μ'', were also measured for toroid-shaped ferrite samples as a function of frequency between 1MHz to 1GHz , the samples having been sintered at 1260°C, 1300°C and 1340°C. Using the dielectric complex-plane plots as the guide, magnetic complex-plane plots were obtained for the imaginary part, μ'', versus the real part, μ', of the permeability. It is suggested that these magnetic analogues of the dielectric complex-plane have a strong potential of being exploited to yield details of magnetic polarization.

Keywords: nickel zinc ferrite; dielectric complex-plane; magnetic complex-plane

INTRODUCTION

Nickel zinc ferrite materials with the spinel structure have been widely used in various electronic devices such as inductors and or transformer cores in the relatively high frequency region because of their high magnetic permeability and high electrical resistivity. The nickel zinc ferrite has both significant dielectric and magnetic properties which vary with frequency, temperature and other variables in a similar manner. The polycrystalline Ni-Zn ferrites have been extensively used in a number of electronic devices due to their sufficiently large permeability at high frequency, remarkably high

resistivity and mechanical hardness, reasonable cost and chemical stability [1]. The high electrical resistivity and good magnetic properties make this ferrite an excellent core material for power transformation in electronic and telecommunication applications [2, 3]. Nickel zinc ferrite is a soft magnetic material having low magnetic coercivity and high resistivity values [4]. The electrical and magnetic properties of Ni-Zn ferrite are sensitive to microstructure (grain size, grain boundary and pores), which is governed by the preparation process. Dielectric studies and analysis have been reported in many literature papers [5]. For several decades, the most common method for preparation of ferrites is by the conventional ceramic technique and many of the findings on their excellent properties were obtained using samples produced by this technique. Although the magnetic and dielectric properties of Ni-Zn ferrite have been reported, but there is no report on any comparative studies of magnetic and dielectric properties of Ni-Zn ferrite, particularly of magnetic complex-plane plot and dielectric complex-plane plot.

METHOD

Ferrites samples with the chemical formula $Ni_{0.3}Zn_{0.7}Fe_2O_4$ were prepared by the conventional solid state method. High purity oxides of NiO(99.99%), ZnO(99.9%) and Fe_2O_3 (99.99%) were mixed together according to their molecular weights. Then, the mixed powders were presintered at 1240°C. After that, the presintered material was crushed by ball milling for 3 hours. The powders were mixed with an appropriate amount of polyvinyl alcohol (PVA) as a binder and zinc stearate as a lubricant to improve the powder flowability. Then, the powders were pressesed into toroidal and discshape. Finally, these samples were sintered at 1260°C, 1300°C and 1340°C. During the sintering process, the PVA binder and zinc stearate would be removed. The density of the sample was determined by the Archimedes method. All the samples were investigated by X-ray diffraction (XRD) to identify phases. Microstructural analysis of the samples was obtained using scanning electron microscopy (SEM). The dielectric and magnetic measurement were performed using an HP4291A Impedance Analyzer in the frequency range 1MHz to 1GHz. Curie temperature measurement was carried out by using an Agilent 4294A Precision Impedance Analyzer.

RESULTS AND DISCUSSIONS

The XRD patterns of the as-prepared and three samples sintered at different sintering temperatures of 1260˚C,1300˚C and 1340˚C are shown in figure 1. The XRD analysis, presented in the figure confirmed the existence of single phase cubic spinel structure with no extra lines corresponding to second phase formation that could be attributed to the presence of unreacted ingredients. As shown in the figure, clear XRD patterns exhibit peaks, confirming the presence of nickel zinc ferrite after a 10 hours sintering.

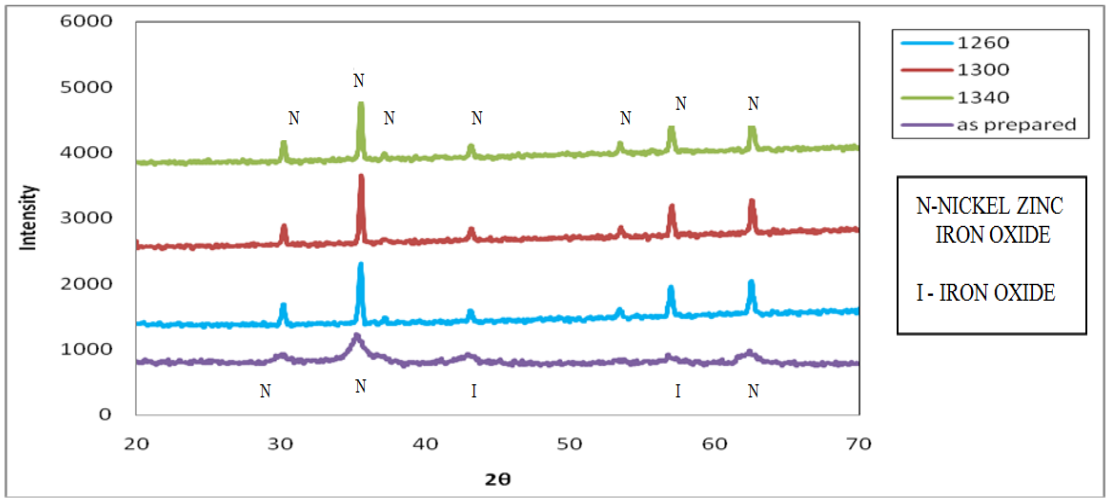

Figure 1: The XRD Patterns of $Ni_{0.3}Zn_{0.7}Fe_2O_4$ sintered at a) 1260°C, b) 1300°C and c) 1340°C

Figure 2 shows a TEM micrograph of the $Ni_{0.3}Zn_{0.7}Fe_2O_4$ powder obtained from the milling process for 3 hours. TEM micrographs were used to obtain the average particle size by sampling about 100 particle images from the micrographs and the average particle size for $Ni_{0.3}Zn_{0.7}Fe_2O_4$ is 102.6nm. Density measurements were conducted on the sintered samples according to the Archimedes principle. The data obtained in these measurements are given in TABLE 1. From the table, the density was found to increase with increasing temperature due to the increase in grain size and diminished pores.

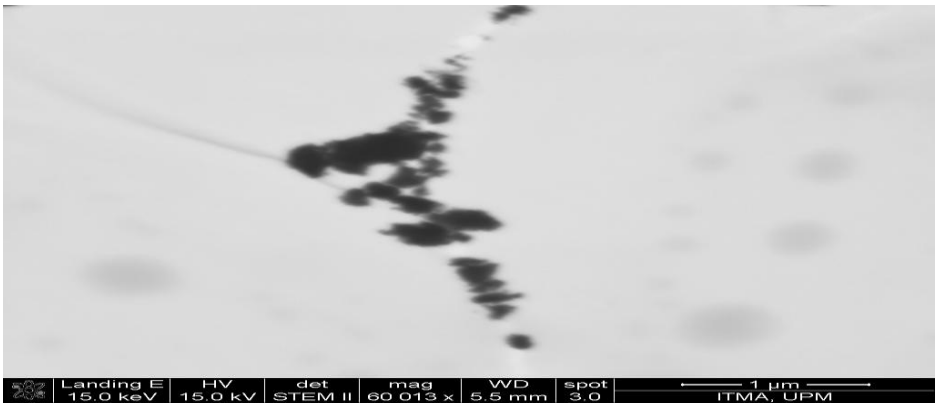

Figure 2: TEM picture

Table 1: Density measurement for samples sintered at1260°C, 1300°C and 1340°C

Sintering Temperature (°C)	Density (g/cm^3)
1260	4.645
1300	4.748
1340	4.854

The SEM images of toroid samples sintered at 1260°C, 1300°C and 1340°C sintering temperature are shown in FIGURE 3. From the SEM micrograph, the average grain sizes were observed to be 2.99μm (1260˚C), 3.27μm (1300˚C) and 4.80μm (1340˚C). The increase in grain size with increasing sintering temperature is clearly visible for the samples. This is due to the grain growth during the sintering process. When the sintering temperature increased, the average grain size and density increased indicating that the microstructure had become more compact with less grain boundaries and reduced discontinuity between the grains. It shows that the sample with the sintering temperature 1340°C has larger grain size and has higher complex permeability and complex permittivity.

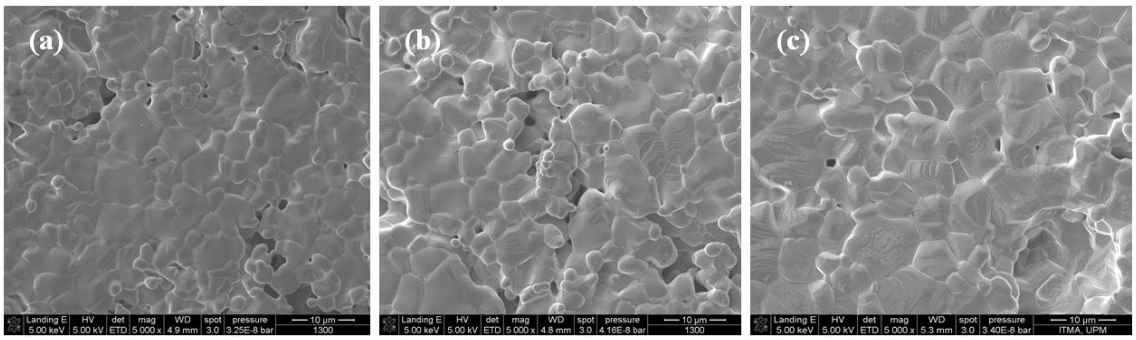

Figure 3: SEM images of toroid samples sintered at (a) 1260°C, (b) 1300°C and (c) 1340°C

The dielectric constant and dielectric loss of $Ni_{0.3}Zn_{0.7}Fe_2O_4$ were studied in a frequency range from 1MHz to 1GHz at room temperature shown in figure 3(a). Obviously, the dielectric constant and dielectric loss increased with sintering temperature and decreased with increasing frequency. Above certain frequencies, the value of dielectric constant, ε' and dielectric loss, ε'' became much lower. This dispersion occurs because beyond a certain frequency of the externally applied electric field, the electron hopping or electron exchange between Fe^{2+} and Fe^{3+} cannot follow the alternating field. Thus the dielectric constant, ε' and dielectric loss, ε'' decreased at high frequency. Both the dielectric constant and dielectric loss were seen to increase with increasing sintering temperature. It is known that an increase in sintering temperature leads to an increase in Fe^{2+} concentration and is therefore, responsible for the increase in polarization. Furthermore the increase in grain size causes an increase in the grain to grain boundary thickness ratio, which is responsible for the increase in permittivity (dielectric constant and dielectric loss). Thus, the sample sintered at 1360°C had the biggest average grain size and displayed the highest permittivity. Figure 3(b), showed the dielectric loss, ε'', plotted as a function of dielectric constant, ε', which gives the dielectric complex-plane plot. From that plot, it is seen that the dielectric properties in this sample arises from the bulk (grain) and the grain boundary, with the frequency decreasing towards the right of the plot. At low and high frequency the properties are interpreted as mainly due to interfacial and dipolar polarization

respectively. At low frequency, the polarization is mainly interfacial polarization, which is due to the accumulation of charges at the grain boundary; an increase in polarization results in more and more charges reaching the grain boundary with increasing frequency. In general, the grains have a higher value of permittivity, while the grain boundaries have lower values. However, at lower frequencies, the grain boundaries account more for the permittivity than the grains due to interfacial polarization. Therefore permittivity is high at lower frequencies and decreases as frequency increases.

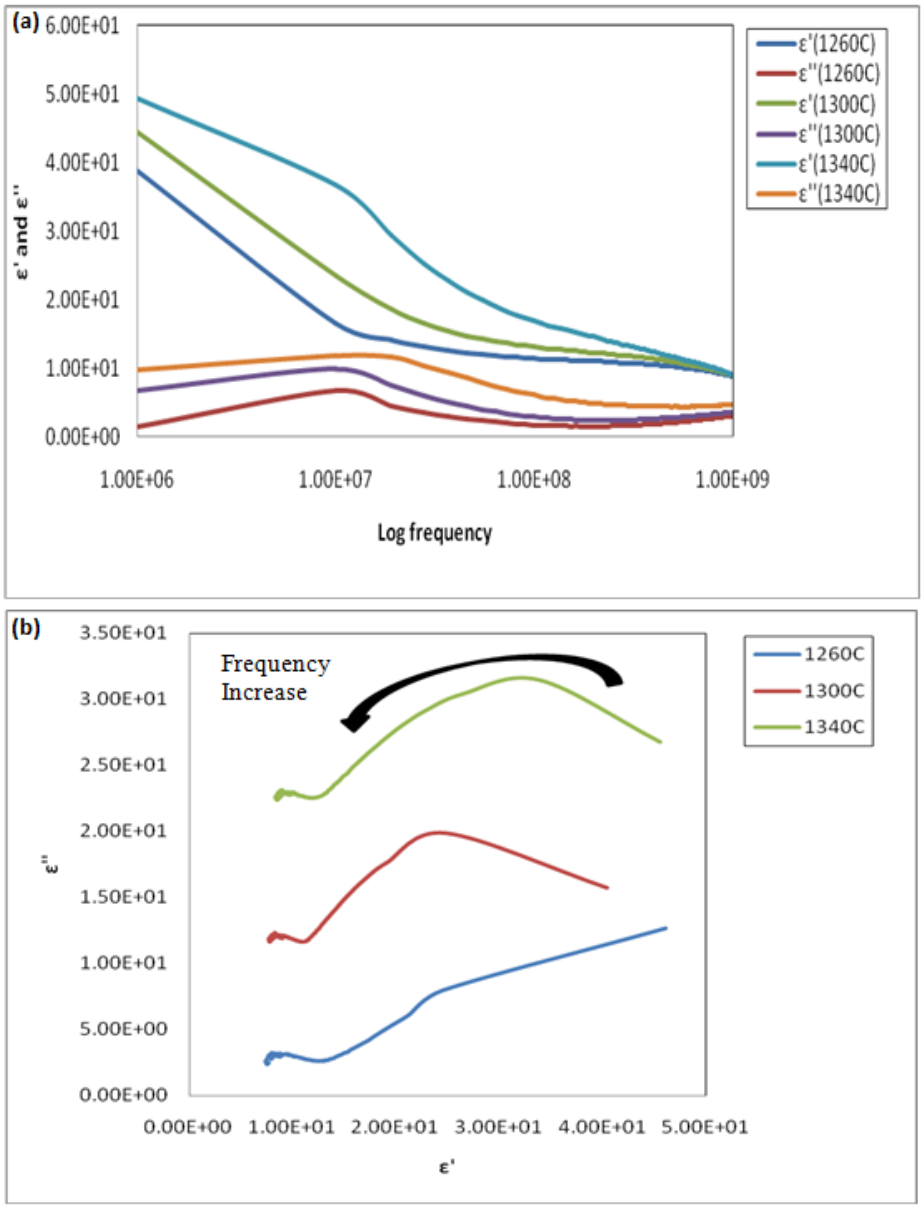

Figure 3: (a) frequency dependence of dielectric constant and dielectric loss and (b) Dielectric Complex-Plane plot

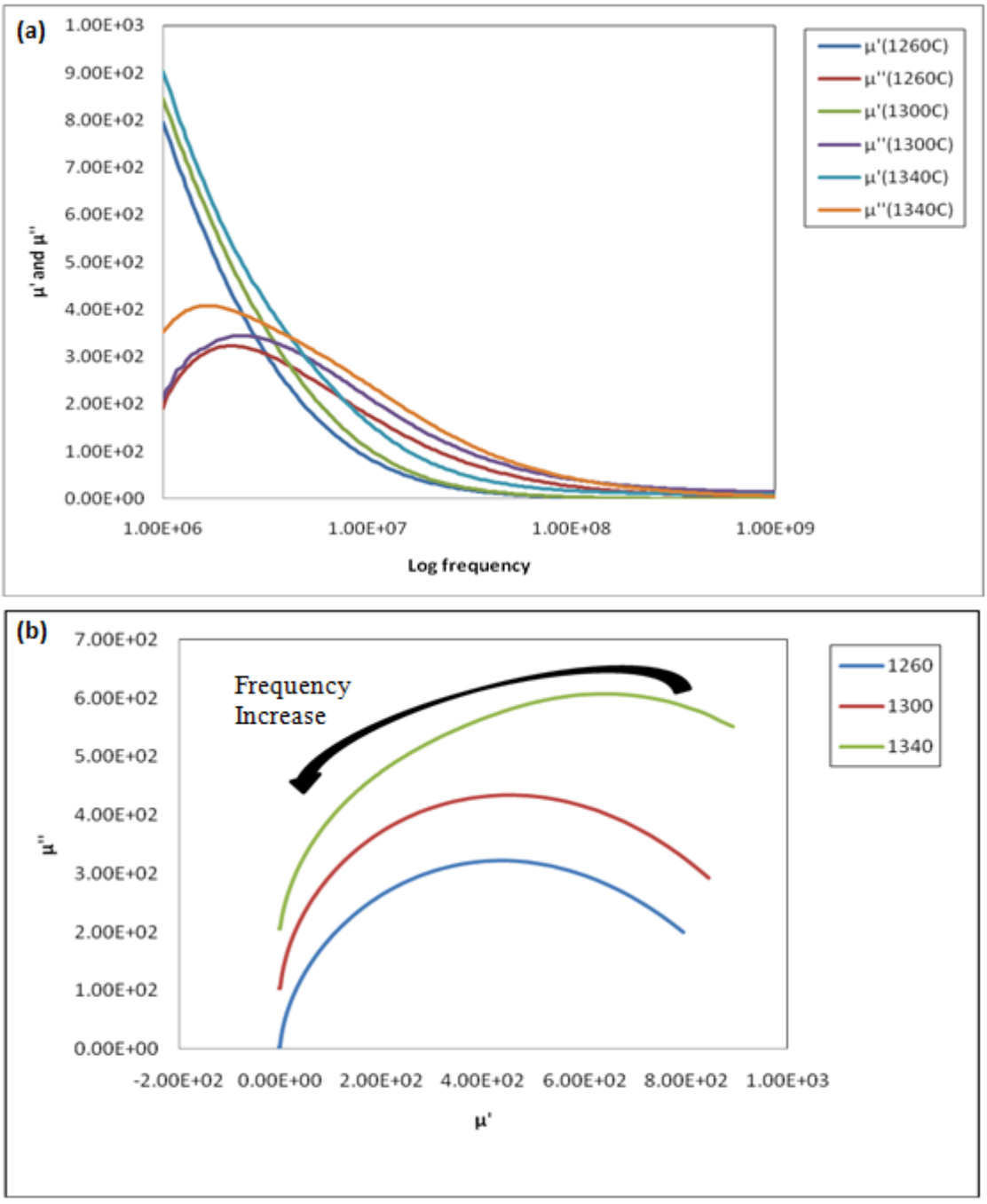

Figure 4: (a) frequency dependence of real and imaginary part of permeability (b) Magnetic Complex-Plane plot

Figure 4 (a) show variations in the real part,μ', and imaginary part,μ'', of permeability as a function of frequency at room temperature for the samples sintered at 1260°C, 1300°C and 1340°C. From the figure it shows that the real part of permeability, μ', decreases rapidly with increasing frequency. The imaginary part of permeability, μ'' gradually increases with the frequency, takes a broad maximum at certain frequencies and then decreases rapidly. This feature is well known as the natural resonance. At the natural resonance frequency the Larmor frequency of spins is equal to the external magnetic-field frequency. Thus at this frequency, the spin moments strongly absorb the magnetic energy which is carried by the oscillating magnetic field. At this point the permeability will attain the highest possible value. At frequencies above this value, there will be a lag between the applied field frequency and the movement of the domain spins. At higher frequencies, losses are found to be lower because of the domain wall motion is inhibited and the magnetization is forced to change by rotation. The increase of losses with increase in sintering temperature and consequently in the number and size of magnetic domains contribute to loss due to delay in domain wall motion. The real part of permeability, μ', and imaginary part of permeability, μ'' increase with increasing sintering temperature. This phenomenon is attributed to the contribution of domain wall motion which becomes more significant as the sintered density and grain size of the ferrite increase; the sample sintered at 1340°C which was sintered at the highest sintering temperature and had the biggest average grain size displayed the highest permeability. The higher the density and grain size the greater the grain to grain continuity of magnetic flux leading to higher permeability. FIGURE 4 (b) shows complex-plane permeability plots for sintering temperatures 1260°C, 1300°C and 1340°C. From the plots, the magnetic response in the samples was dominated by domain wall movement only because the samples contain domains due to large average grain size and as a result the magnetization process occurs primarily by domain wall movement and less by domain rotation. Thus the complex-plane permeability can be interpreted to show a magnetic domain wall response (magnetic polarization process due to domain walls displacements)

The variation of permeability with temperature was measured for the sintered ferrites at a constant frequency of 10kHz in the temperature range from (room tempearture to 100°C) shown in figure 5. This figure it shows the permeability falling sharply when the magnetic state of the ferrite samples changes from being ferromagnetic to being paramagnetic. The permeability would increase gradually with increase of the temperature until achieving certain temperature (peak point). After this peak point, the permeability drops dramatically and this temperature is called the curie temperature.The heat treatment did not effect the crystal structure of the nickel zinc ferrite. So we can say that, the curie temperature for the nickel zinc ferrite remained the same for the three sintering temperatures. Any change of the curie temperature would be due to a change in the exchange force between moments arising from a change of the crystal structure of the sample. These however did not occur since the curie temperature value remained constant for all the sintering temperatures.

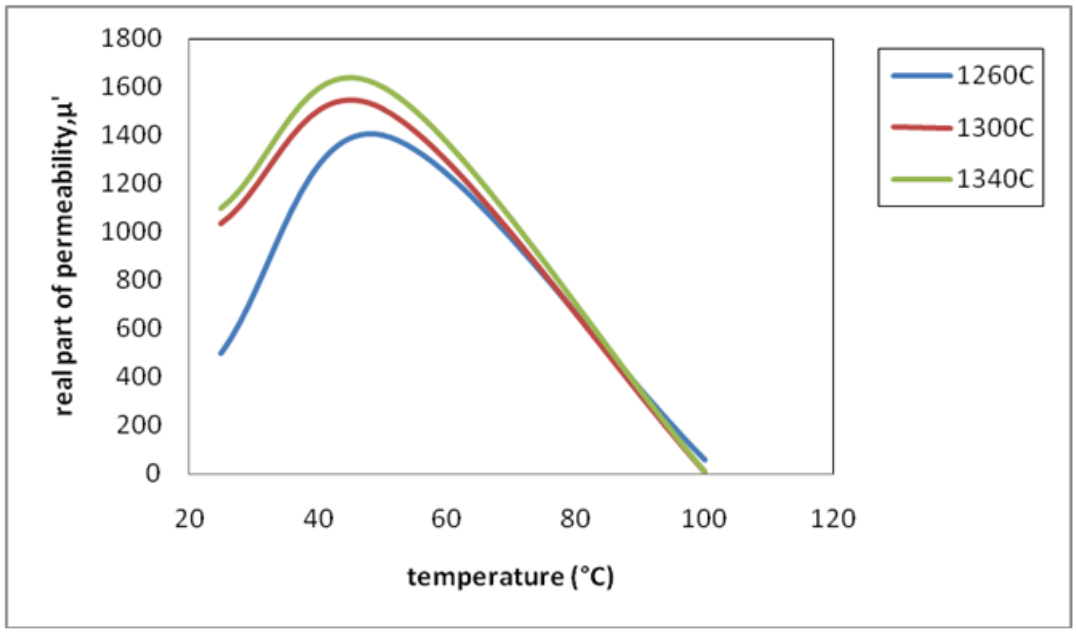

Figure 5: variation of the real part of permeability with temperature

CONCLUSION

The samples sintered at different temperatures were characterized in terms of dielectric constant, dielectric loss and dielectric complex-plane plot as well as the real part of permeability, imaginary part of permeability and magnetic complex-plane plot. The Curie temperature was found to be constant for all the samples sintered at the various temperatures. The dielectric complex-plane plot is used to describe the relation between dielectric constant and dielectric loss over the entire frequency range when temperature is constant. From the dielectric complex-plane plot, the dielectric polarization was contributed by the interfacial and dipolar polarization. The magnetic complex –plane plots are plotted as guided by the dielectric case to describe the relation between real part of permeability and imaginary part of permeability over the entire frequency range when temperature is constant. The mechanism of magnetization is discussed, the magnetization process was probably dominated by magnetic domain wall movement only.

ACKNOWLEDGMENTS

The authors are grateful to Universiti Putra Malaysia for Research University Grant (vote number 05-04-08-0548RU)

REFERENCES

[1]. Ishino. K, Narumiya. Y, *Ceram. Bull.* **66** (1987) 1469
[2]. Slick. P.I, in:E.P.Wohlfafth(Ed), Ferrogmagnetic Materials, Vol 2, North-Holland Pub.Co., Amsterdam, 1980,p.196

[3]. Abraham. T, *Am.Ceram.Bull.Soc.Bull.* **73** (1994) 62-65
[4]. Kumar. P.S.A., Shontri. J.J., Kulkani. S.D., Deshpande. C.D., Date. S.K., *Mater.Lett.* **27** (1996) 293-296.
[5]. Jonsher, A. K. (1983). *Dielectric Relaxation In solids*: Chelsea Dielectric Press London.